Reaction Mechanism and Tautomeric Equilibrium of 2-Mercaptopyrimidine in the Gas Phase and in Aqueous Solution: A Combined Monte Carlo and Quantum Mechanics Study

Maria Carolina P. Lima,[†] Kaline Coutinho,[‡] Sylvio Canuto,[‡] and Willian R. Rocha*[,†,§]

Departamento de Química Fundamental - CCEN, Universidade Federal de Pernambuco, 50670-901, Cidade Universitária, Recife, PE, Brazil, Instituto de Física, Universidade de São Paulo, CP 66318, 05315−970, São Paulo, SP, Brazil, and Departamento de Química, ICEX, Universidade Federal de Minas Gerais, 31270-901 Pampulha, Belo Horizonte, MG, Brazil

Received: February 8, 2006; In Final Form: April 13, 2006

A combined Monte Carlo and quantum mechanical study was carried out to analyze the tautomeric equilibrium of 2-mercaptopyrimidine in the gas phase and in aqueous solution. Second- and fourth-order Møller−Plesset perturbation theory calculations indicate that in the gas phase thiol (Pym-SH) is more stable than the thione (Pym-NH) by ca. 8 kcal/mol. In aqueous solution, thermodynamic perturbation theory implemented on a Monte Carlo *NpT* simulation indicates that both the differential enthalpy and Gibbs free energy favor the thione form. The calculated differential enthalpy is $\Delta H_{SH\rightarrow NH}(solv) = -1.7$ kcal/mol and the differential Gibbs free energy is $\Delta G_{SH\rightarrow NH}(solv) = -1.9$ kcal/mol. Analysis is made of the contribution of the solute−solvent hydrogen bonds and it is noted that the SH group in the thiol and NH group in the thione tautomers act exclusively as a hydrogen bond donor in aqueous solution. The proton transfer reaction between the tautomeric forms was also investigated in the gas phase and in aqueous solution. Two distinct mechanisms were considered: a direct intramolecular transfer and a water-assisted mechanism. In the gas phase, the intramolecular transfer leads to a large energy barrier of 34.4 kcal/mol, passing through a three-center transition state. The proton transfer with the assistance of one water molecule decreases the energy barrier to 17.2 kcal/mol. In solution, these calculated activation barriers are, respectively, 32.0 and 14.8 kcal/mol. The solvent effect is found to be sizable but it is considerably more important as a participant in the water-assisted mechanism than the solvent field of the solute−solvent interaction. Finally, the calculated total Gibbs free energy is used to estimate the equilibrium constant.

I. Introduction

Tautomerism is an essential ingredient in several chemical and biochemical processes. Understanding tautomeric reactions is very important in biological mechanisms and this is a strong motivation for theoretical studies. In particular, the role played by the solvent is known to be crucial. Among all possible solvents, water is the natural biological solvent and is involved in all processes related to life. Investigations of tautomeric reactions in an aqueous environment is a great theoretical challenge and this is the subject of this work. We address a systematic investigation of the relative stability and the reaction mechanisms of 2-mercaptopyrimidine in aqueous solution using a combination of quantum mechanics and computer simulation of liquids.

Mercaptopyrimidines are thio derivatives of pyrimidine and play an important role in several important biological processes, as for example, antiviral, antibacterial, antitumor and antithyroidal activities.[1] This heterocyclic compound is usually involved in tautomeric equilibrium of the type thiol/thione (Pym-SH/Pym-NH), as shown in Scheme 1, and pyrimidine/pyrimidone, when sulfur is replaced by oxygen, which has important biological consequences. For example, the mutation during DNA replications may be correlated with the tautomerism of purine and pyrimidine bases, causing a wrong pairing of the DNA bases.[2] 2-Mercaptopyrimidine also exhibits a rich coordination chemistry,[3] possessing the ability to coordinate to a single or several transition metal centers in different ways. As a result of the tautomerism of this compound, the coordination ability and also the biological activities of the resulting coordination compounds will be influenced.[4]

SCHEME 1

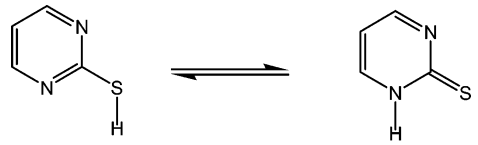

Pym-SH **Pym-NH**

Most of our current understanding of the tautomerism involving heterocyclic compounds has been based on detailed studies involving pyridines and pyrimidines substituted with SH or OH groups at the 2 or 4 positions.[5] These studies have shown that the predominant form present in equilibrium is largely dependent on environmental effects. Thus, X-ray diffraction studies[6] revealed that in the solid state 2-mercaptopyridine exists predominantly as hydrogen-bonded (HB) dimers of the thione form. It has also been demonstrated by UV spectroscopy[7] that polar solvents and self-association shift the tautomeric equilibrium significantly toward the thione form. But in dilute solution

* Corresponding author. E-mail: wrocha@ufmg.br. Permanent Address: Departamento de Química, ICEX, Universidade Federal de Minas Gerais, 31270-901, Belo Horizonte, MG, Brazil.
[†] Universidade Federal de Pernambuco.
[‡] Universidade de São Paulo.
[§] Universidade Federal de Minas Gerais.

10.1021/jp060821b CCC: $33.50
Published on Web 05/16/2006

or nonpolar solvents, the thiol form predominates. ^{1}H NMR studies[8] in a number of solvents of different polarities and hydrogen bonding character also revealed that 2-mercaptopyrimidine exists predominantly in the thione form as hydrogen-bonded monomers or dimers. On the other hand, gas phase IR investigations in an argon matrix[9] of 2-mercaptopyrimidine showed that the thiol form predominates in the gas phase. This is corroborated by mass spectrometry[10] and photoelectron spectroscopy[11] studies in the gas phase of both 2- and 4-mercaptopyridines.

The thiol/thione and lactim/lactam tautomeric equilibrium has also attracted some theoretical interest because this is a suitable system to test the applicability of different computational methods and solvation theories. Thus, the tautomeric equilibrium involving pyridines and pyrimidines substituted with SH or OH groups at the 2 position has been studied theoretically[9,12] with varying degrees of sophistication, ranging from semiempirical,[12a,d,e] density-functional (DFT) methods,[12g,h] and ab initio Hartree−Fock (HF), second-order Møller−Plesset perturbation (MP2) and configuration interaction (CI) calculations.[9,12b,f,g] The effect of the solvent on the tautomeric equilibrium has been investigated by means of reaction field theories[12f,g] and statistical mechanical simulations.[12c] The theoretical studies are, in general, in line with the experimental findings and have also revealed that the tautomeric equilibrium is drastically affected by basis set and electron correlation effects.[12g]

Despite the extensive results on the isolated species, the free energy of solvation, relative stability and the mechanism by which the proton is transferred from one tautomer to another in 2-mercaptopyrimidine (Scheme 1) is still unclear. Kinetic experiments on the tautomeric equilibrium involving the 2-hydroxypyridine[13] have shown that in aprotic media, the tautomeric interconversion takes place through an intermolecular proton transfer mechanism, within the self-associated monomers. In contrast, in aqueous solution the kinetic experimental data exclude the self-association mechanism and a solvent-assisted mechanism is proposed, in which one or more water molecules act as a bifunctional catalyst.[14] Following these experimental studies, Lledós and Bertrán,[12a] employing the semiempirical CNDO/2 method, showed that the tautomeric interconversion of 2-hydroxypyridine, with the assistance of one water molecule leads to a proton transfer reaction without an energy barrier. Later theoretical work performed by Scanlan and Hillier,[12b] on this same system, in the gas phase, at the HF/3-21G level, showed that in the mechanism involving a self-associated dimer the barrier is reduced by ca. 35 kcal/mol, compared to the direct intramolecular mechanism.

From the previous experimental and theoretical studies it can be inferred that, opposite to the gas phase, the thione form is more stable in water than the thiol form. But this still needs not only a theoretical or experimental corroboration but also an estimate of the relative energy between the two tautomeric forms in the gas phase and in aqueous solution. As to the possible thiol Pym-SH → thione Pym-NH interconversion mechanism, two possibilities need detailed investigations. One is the natural candidate of a direct mechanism of proton transfer. The other is the conversion with the water assisted mechanism with the participation of one water molecule. These are the major interest of this work.

In this work a combination of Monte Carlo (MC) simulations and quantum mechanical calculations was carried out to perform a thorough analysis of the tautomeric equilibrium of 2-mercaptopyrimidine in the gas phase and in aqueous solution. The stability of the species in the gas phase and in aqueous solution, the factors governing the preferential solvation of the species, and hydrogen bond analysis of the solvated tautomers are analyzed. The proton transfer reaction was investigated by assuming two distinct mechanisms: a direct intramolecular proton transfer mechanism and a solvent-assisted mechanism. The Gibbs free energy calculations and the inclusion of solvent effects along the reaction coordinates are made by means of thermodynamic perturbation theory.[15]

TABLE 1: Intermolecular Parameters Used in the Monte Carlo Simulations (q in Elementary Charge Unit, ϵ in kcal/mol, and σ in Å)

			q	
interaction site	σ	ϵ	Pym-SH	Pym-NH
N1	3.250	0.170	−0.743	−0.365
C2	3.750	0.110	0.547	0.255
C3	3.750	0.110	−0.499	−0.492
C4	3.750	0.110	0.484	0.629
N5	3.250	0.170	−0.635	−0.681
C6	3.750	0.110	0.777	0.612
S	3.550	0.250	−0.299	−0.431
H8	0.000	0.000	0.009	−0.029
H9	0.000	0.000	0.157	0.164
H10	0.000	0.000	0.005	0.101
H11	0.000	0.000	0.197	0.237
water				
O	3.15061	0.15210	−0.834	
H	0.000	0.000	0.417	

II. Theoretical Details

Full geometry optimization and vibration frequency calculations in the gas phase were performed at the MP2 level of theory, within the frozen core approach, employing the split-valence 6-31++G(d,p)[16] basis set, which includes diffuse and polarization functions in all atoms.[17] Aiming at obtaining better energetic results for the isolated species, single point calculations at the MP4 level of theory with single, double, triple and quadruple substitutions, MP4(SDTQ), were performed on the optimized MP2/6-31++G(d,p) structures, with the same basis set. To study the differential solvation of the Pym-NH and Pym-SH forms of 2-mercaptopyrimidine in water, we have carried out MC statistical mechanical simulation, in the isobaric−isothermal (NpT) ensemble at $T = 298$ K and $p = 1$ atm. Standard procedures,[18] including the Metropolis sampling technique[19] and periodic boundary conditions combined with the image method in a cubic box were used. The intermolecular interactions were described by the Lennard-Jones (LJ) plus Coulomb potential, with three parameters for each atom i (ϵ_i, σ_i and q_i) and a combination of $\epsilon_{ij} = (\epsilon_i\epsilon_j)^{1/2}$ and $\sigma_{ij} = (\sigma_i\sigma_j)^{1/2}$. The sets of intermolecular parameters used in the simulations are shown in Table 1. For water, the TIP3P[20] potential is used. For the tautomeric species, all atoms are described by the OPLS parameters[21] with the charges calculated using the ChelpG fitting procedure[22] at the MP2/6-31++G(d,p) level of theory. The intermolecular interactions have been truncated at a cutoff distance of 10.8 Å, and the long-range corrections to the LJ interactions have been included using the pair radial distribution function procedure.[18] In every simulation the Pym-NH and Pym-SH forms of 2-mercaptopyrimidine were held rigid. The simulation consisted of 1 solute molecule (Pym-NH or Pym-SH) plus 343 water molecules. One MC step is concluded after selecting one molecule randomly and trying to translate it in all directions and also trying to rotate it around a randomly chosen axis. The maximum displacement of the molecules has been self-adjusted to give an acceptance ratio around 50%. Attempts to change the volume were made every 1000 MC

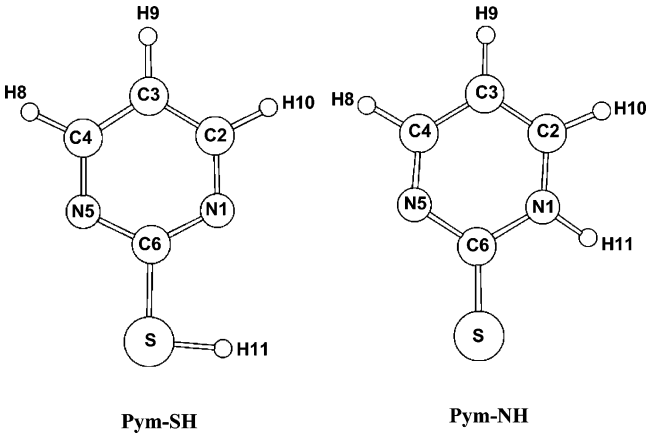

Figure 1. Optimized MP2/6-31++G(d,p) structure for the thiol (Pym-SH) and thione (Pym-NH) forms of 2-mercaptopyrimidine, showing the atomic labels.

steps. After the equilibration phase, the simulations consisted of 3.4×10^7 MC steps, corresponding to 10^5 MC steps per molecule.

To investigate the proton transfer reaction in solution, we have used the following two-step approach. First, the reaction path for the proposed mechanisms is obtained in the gas phase by employing the combined relaxed path algorithm developed by Ayala and Schlegel.[23] This procedure locates the transition state and reaction path connecting two structures, combining geometry optimization techniques, the quadratic synchronous transit guided approach[24] and the Gonzalez−Schlegel algorithm for the reaction path following.[25] After obtaining the gas phase reaction path, the free energy profile in solution is obtained by perturbing one structure into the nearest structure along the gas phase reaction path by using thermodynamic perturbation theory.[15] The free energy difference in solution between structures *i* and *j*, $\Delta G_{i\rightarrow j}$(solv), is then calculated according to the equation

$$\Delta G_{i\rightarrow j}(\text{solv}) = -k_B T \ln\langle \exp[-(H_j - H_i)/k_B T]\rangle_i \qquad (1)$$

where H_i is the conformational enthalpy and the averaging is for sampling based on structure *i* in solution. Further details of the free energy perturbation are given in the next section discussing the free energy of solvation and the tautomeric interconversion in solution. All ab initio calculations reported here have been carried out using the program Gaussian 98,[26] and the Monte Carlo simulations have been performed with the DICE program.[27]

III. Results and Discussions

A. Isolated Species in the Gas Phase. The MP2/6-31++G(d,p) optimized structures for the thiol (Pym-SH) and thione (Pym-NH) forms of 2-mercaptopyrimidine are shown in Figure 1, and the structural parameters are quoted in Table 2. Unfortunately, the experimental geometries of the tautomers are not known. However, the experimental structure of the solid state 2-mercaptopyridine, which exists as a hydrogen-bonded dimer of the thione form, is known from X-ray and neutron diffraction experiments[6] and is also shown in Table 2. As can be seen, the optimized parameters of the Pym-NH form of 2-mercaptopyrimidine are not much different from the experimental geometry of 2-mercaptopyridine. As the experimental results for the C=S and N−H bond distance are for the hydrogen-bonded dimers, it is to be expected that these are slightly larger than for the isolated Pym-NH tautomer. Indeed, the calculated C=S bond length of 1.649 Å computed for the Pym-NH tautomer correlates well with the experimental value for the hydrogen-bonded dimer of 1.692 Å for 2-mercaptopyridine. The corresponding value for 2-thiouracil[28] is 1.669 Å. The N−H bond distance of 1.014 Å computed for the Pym-NH tautomer is also slightly decreased compared to the experimental value of 1.041 Å for the 2-mercaptopyridine dimer, as expected. The computed bond angles are also in line with the experimental values.

TABLE 2: Optimized MP2/6-31++G(d,p) Structural Parameters of the Thiol and Thione Tautomers of 2-Mercaptopyrimidine[a]

bond length (Å)	Pym-SH	Pym-NH	bond angles (deg)	Pym-SH	Pym-NH
N1−C2	1.344	1.357 [1.354(3)]	N1−C2−C3	122.5	118.8
C2−C3	1.393	1.369 [1.352(4)]	C2−C3−C4	116.6	116.1
C3−C4	1.394	1.421	C3−C4−N5	122.5	125.1
C4−N5	1.343	1.319	C4−N5−C6	115.7	119.4
N5−C6	1.346	1.388	N5−C6−N1	127.0	115.8
C6−S	1.764	1.649 [1.692(2)]	N1−C6−S	118.4	120.2 [120.6(2)]
S−H11	1.333		C6−S−H11	93.8	
N1−H11		1.014 [1.041(2)]	C6−N1−H11		114.9 [121.0(10)]

[a] Values in brackets were taken from the X-ray diffraction experiments on dimers of 2-mercaptopyridine.[6]

TABLE 3: Computed Energies and Dipole Moment of the Isolated Thiol and Thione Tautomers of 2-Mercaptopyrimidine in the Gas Phase[a]

	Pym-SH	Pym-NH
$E_{tot.}$(MP2)	−661.1981035	−661.1861833
E^{ZPE} [b]	0.076256	0.079143
H[b]	0.083259	0.086035
G[b]	0.045947	0.048259
μ[b]	3.08	6.87
$E_{tot.}$(MP4(SDTQ)//MP2)	−661.2838344	−661.2728511
$\Delta E_{SH\rightarrow NH}$(MP2)	7.5	
$\Delta E^{ZPE}_{SH\rightarrow NH}$(MP2)	9.3	
$\Delta H_{SH\rightarrow NH}$(MP2)	9.2	
$\Delta G_{SSH\rightarrow NH}$(MP2)	8.9	
$\Delta E_{SH\rightarrow NH}$(MP4(SDTQ)//MP2)	6.9	
$\Delta E^{ZPE}_{SH\rightarrow NH}$(MP4(SDTQ)//MP2)	8.7	
$\Delta H_{SH\rightarrow NH}$(MP4(SDTQ)//MP2)	8.6	
$\Delta G_{SH\rightarrow NH}$(MP4(SDTQ)//MP2)	8.3	

[a] All calculations were performed with the 6-31++G(d,p) basis set. [b] Values of E^{ZPE}, H and G are given in au and dipole moment (μ) in units of Debye. Energy differences are given in kcal/mol.

The absolute and relative energies, $\Delta E_{SH\rightarrow NH}$, for the gas phase process Pym-SH → Pym-NH are shown in Table 3. As can be seen, in the gas phase the thiol form is more stable than the thione form in all levels of theory studied. At the MP2 level of theory, the thiol species is 7.5 kcal/mol more stable than the thione tautomer; i.e., the tautomeric equilibrium is shifted to the thiol form. Inclusion of zero point vibrational energy (ZPE) increases the $\Delta E_{SH\rightarrow NH}$ by 1.8 kcal/mol, still in favor of the thiol Pym-SH form. Table 3 also gives the values of $\Delta H_{SH\rightarrow NH}$ and $\Delta G_{SH\rightarrow NH}$. These indicate a small contribution of the entropy in the gas phase, as expected. To ascertain the accuracy of the MP2 results, MP4(SDTQ)//MP2 values are also reported. The MP4 value of $\Delta G_{SH\rightarrow NH} = 8.3$ kcal/mol will be taken as our reference value in the gas phase. These results, showing that the thiol form (Pym-SH) is favored over the thione form (Pym-NH) in the gas phase, are in agreement with experiments.[9−11]

Overall, the present theoretical results indicate that in the gas phase the thiol form is favored by ca. 8 kcal/mol.

B. Species in Aqueous Solution. *1. Differential Hydration Enthalpy.* We now consider the differential hydration between the thiol and thione forms without consideration of the possible mechanisms involved in the interconversion. This is obtained by calculating the enthalpy of hydration of both Pym-SH and Pym-NH. We calculate the difference in enthalpy using

$$\Delta H_{SH\rightarrow NH}(solv) = \Delta E_{SH\rightarrow NH}(solv) - p\Delta V_{SH\rightarrow NH}(solv) \quad (2)$$

where

$$\Delta E_{SH\rightarrow NH}(solv) = \Delta E^{XS}_{SH\rightarrow NH}(solv) + \Delta E^{SS}_{SH\rightarrow NH}(solv) \quad (3)$$

with XS denoting the solute−solvent and SS denoting the solvent−solvent interaction.[29]

MC simulations were carried out on aqueous solutions of the isolated species to analyze the preferential solvation of the tautomers and to compute the free energy of solvation of each species. The densities of both systems were obtained as 1.015 ± 0.005 g/cm^3, which gives a negligible difference of the thermodynamic term $p\Delta V_{SH\rightarrow NH}(solv)$ in solution. Therefore, the difference of the enthalpy in solution was found as $\Delta H_{SH\rightarrow NH}(solv) = \Delta E_{SH\rightarrow NH}(solv) = -1.71 \pm 0.52$ kcal/mol, indicating the preferable hydration of the thione form. The differential enthalpy of hydration is composed of two parts where $\Delta E^{XS}_{SH\rightarrow NH}(solv) = -11.00$ kcal/mol and $\Delta E^{SS}_{SH\rightarrow NH}(solv) = 9.29$ kcal/mol. The solute−solvent interaction energies, E^{XS}, computed separately for Pym-NH and Pym-SH are respectively −34.02 and −23.02 kcal/mol ($\Delta E^{XS}_{SH\rightarrow NH}(solv) = -11.00$ kcal/mol), which shows that in aqueous solution the thione form interacts more strongly with water. This would be expected because the thione form has a greater dipole moment than the thiol form. The difference of the solvent−solvent interaction energies, ΔE^{SS}, computed for the water molecules around Pym-NH and Pym-SH ($\Delta E^{SS}_{SH\rightarrow NH}(solv) = 9.29$ kcal/mol), shows that the reorganization of the water molecules favors their interaction in the presence of thiol than in the presence of thione. This indicates that the reorganization of the solvent plays an important role in the stabilization of the two tautomeric forms in solution.

As a general result, we find here that the hydration enthalpy of the thione Pym-NH form is larger than the thiol Pym-SH form by ca. 1.7 kcal/mol. Experimentally,[7,8] it is indeed expected that the thione form is favored in water in contrast to the gas phase situation.

2. Structural Properties and Hydrogen Bonds. The result that in aqueous solution thione stabilizes better than thiol can also be seen in the local hydrogen bond (HB) shell. In this subsection we analyze the hydrogen bond sites and the corresponding interaction of water with thione and thiol. Hydrogen bonds are identified using the structural and energetic criteria.[30] We consider here that a hydrogen bond is formed between the tautomer and water when the distance from the proton donor (D) to the proton acceptor (A) is $R_{D-A} \leq 3.6$ Å, the angle $\theta_{A-HD} \leq 30°$ and the binding energy ≥ 1.0 kcal/mol. These geometric conditions were taken from the radial and angular distributions and the energetic criterion is taken from the pairwise energy distribution, as discussed in several previous publications.[30c−h] Having identified the hydrogen bonds, the average interaction energy is obtained (see Table 4). The average energy for the hydrogen bond in the sulfur atom in Pym-NH that acts as a hydrogen bond acceptor is −3.27 kcal/mol. The hydrogen bonds formed between the nitrogen atoms and water are of the same magnitude, being −3.84 kcal/mol for N5 (HB acceptor) and −3.76 kcal/mol for N1 (HB donor). It is interesting to note that the atoms covalently bound to the H11 (S in thiol and N1 in thione) lose their ability to form hydrogen bonds as proton acceptor, with the SH and NH groups acting only as proton donor. Table 4 summarizes these results and shows that the hydrogen bonds formed between the thione form and the water molecules are stronger than that formed with the thiol form. This observation indicates that the hydrogen bond interaction between the solute and the solvent is consistent with the previous result that in aqueous solution the thione form interacts more strongly with water.

TABLE 4: Average Energy (kcal/mol) of the Hydrogen Bond Interactions between the Two Tautomeric Species and the Water Molecules Obtained in the Configurations Generated by the Monte Carlo Simulations

atomic site	Pym-SH	Pym-NH
N5	−3.26 ± 0.90	−3.84 ± 1.38
S		−3.27 ± 1.04
N1	−3.60 ± 0.75	
H11	−2.52 ± 1.16	−3.76 ± 1.24

3. Differential Free Energy of Hydration. To better understand the differential solvation of the tautomeric species, the free energies of hydration of Pym-NH and Pym-SH were calculated using a hypothetical process[15b] in which the solute is annihilated (meaning that the intermolecular potential parameters of the species X are zeroed: $X \rightarrow 0$) in the ideal gas phase, computing the $\Delta G_{X\rightarrow 0}(gas)$, and in solution, computing the $\Delta G_{X\rightarrow 0}(solv)$. Both variations of free energy are calculated using thermodynamic perturbation theory as described in eq 1. For the simple case where the solute has no internal degrees of freedom, then $\Delta G_{X\rightarrow 0}(gas) = 0$ and the free energy of solvation can be expressed as

$$\Delta G_X(solv) = -\Delta G_{X\rightarrow 0}(solv) \quad (4)$$

For each tautomeric species X, it was necessary to have a series of five simulations using the double-wide sampling,[15c] to make the solute X gradually disappear. As in a previous study,[31] this process was divided into three stages, separately scaling to zero the three parameters of the LJ and Coulomb potential, q_i, ϵ_i and σ_i. First, the Coulomb potential is vanishing by scaling to zero the atomic charges, q_i. The scale factors were $\lambda = 1.0$, 0.9, 0.8, 0.6, 0.4, 0.2 and 0.0. Therefore, using the double-wide sampling in a simulation performed with λ_i (example $\lambda_i = 0.9$), the atomic charges of the solute can be perturbed simultaneously to λ_{i-1} and λ_{i+1} (example $\lambda_{i-1} = 1.0$ and $\lambda_{i+1} = 0.8$). Thus, in total, three simulations were performed ($\lambda_i = 0.9$, 0.6 and 0.2) to vanish the Coulomb potential of the solute. After that, the attractive well of the LJ potential is made to vanish by scaling to nearly zero the atomic parameter ϵ_i. The scale factors were $\lambda = 1.0$, 0.5 and 0.01. In this stage because of the double-wide sampling, only one simulation was performed ($\lambda_i = 0.5$) to remove the attractive well of the LJ potential of the solute. It is interesting to note that at this point, the interaction potential of the solute is described by soft spheres with a repulsive behavior of (σ/r).[12] At the final stage of the annihilation process of the solute, this repulsive potential is vanishing by scaling to zero the atomic parameter σ_i. Only one simulation was performed directly from $\lambda = 1.0$ to 0.0. Changing the sign of this last term of the free energy of solvation gives the cavitation free energy, because in this case only the repulsive potential is made to vanish. Each simulation starts with the last configuration of the previous simulation and it consists of a

TABLE 5: Gibbs Free Energy of Solvation (kcal/mol) for the Two Tautomeric Species Thiol and Thione in Aqueous Solution at 25 °C and 1 atm

		$\Delta G_{\lambda_i \to \lambda_j}$(solv)	
λ_i in q	λ_j in q	Pym-SH	Pym-NH
1.0	0.9	0.889	2.923
0.9	0.8	0.772	2.587
0.8	0.6	1.172	3.799
0.6	0.4	0.804	2.722
0.4	0.2	0.449	1.582
0.2	0.0	0.162	0.616
total of stage 1		4.248	14.230
		$\Delta G_{\lambda_i \to \lambda_j}$(solv)	
λ_i in ϵ	λ_j in ϵ	with $q = 0$	with $q = 0$
1.0	0.5	3.669	3.715
0.5	0.01	5.980	6.100
total of stage 2		9.649	9.815
		$\Delta G_{\lambda_i \to \lambda_j}$(solv)	
λ_i in σ	λ_j in σ	with $q = 0$ and $\epsilon = 1\%$	with $q = 0$ and $\epsilon = 1\%$
1.0	0.0	−2.315	−2.305
total $\Delta G_{X \to 0}$(solv)		11.58 ± 0.56	21.74 ± 0.47
ΔG_X(solv)		−11.58 ± 0.56	−21.74 ± 0.47

SCHEME 2

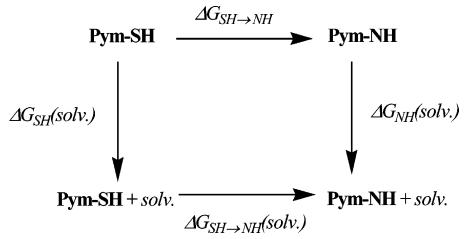

reequilibration phase of 3.4×10^6 MC steps, followed by an average stage of 3.4×10^7 MC steps in the *NpT* ensemble.

The results of the free energy of hydration are summarized in Table 5. The total value obtained to the ΔG_{SH}(solv) is −11.58 ± 0.56 kcal/mol and ΔG_{NH}(solv) is −21.74 ± 0.47 kcal/mol. These results show that in aqueous solution the thione form solvates more than the thiol form, which is in due agreement with the ^{1}H NMR experimental observations.[8] It can be seen in Table 5 that the major difference (around 10 kcal/mol) between the free energy of solvation of the thione and thiol in water comes from the Coulombic part (stage 1) of the potential, reflecting the large difference in the dipole moments of the two forms. As also shown in Table 5, the cavitation free energy of the tautomeric form is nearly the same, i.e., −2.32 and −2.31 kcal/mol, reflecting the small change in the geometry of the two forms.

4. Free Energy of Tautomerization. Additional information that can be obtained is the difference of the free energy of the tautomerization process in solution, $\Delta G_{SH \to NH}$(solv). Using the free energies of solvation of the two tautomeric species (ΔG_{SH}(solv) and ΔG_{NH}(solv)) and the difference of their free energies in the gas phase ($\Delta G_{SH \to NH}$), one can make a thermodynamic cycle, as shown in the Scheme 2 and eq 5.

$$\Delta G_{SH \to NH}(\text{solv}) = \Delta G_{SH \to NH} + \Delta G_{NH}(\text{solv}) - \Delta G_{SH}(\text{solv}) \quad (5)$$

All quantities involved in eq 5 were calculated in the previous sections. The differential free energy of hydration, ΔG_{NH}(solv) − ΔG_{SH}(solv), is −10.16 ± 1.03 kcal/mol, as reported in Table 5. Hence, $\Delta G_{SH \to NH}$(solv) depends now on the choice of $\Delta G_{SH \to NH}$ in the gas phase (Table 3). Using the MP2/6-31++G-(d,p) value, we obtain $\Delta G_{SH \to NH}$(solv) = −1.26 ± 1.03 kcal/mol. At the higher level of MP4//MP2/6-31++G(d,p) we obtain $\Delta G_{SH \to NH}$(solv) = −1.86 ± 1.03 kcal/mol in aqueous solution. All these values are obtained directly from the differential free energy and hence are obtained without assuming any mechanism (or path) for the tautomerization process. These results show that the tautomerization process of the thiol changing to thione form is favorable in water solution, which is again in agreement with the experimental observations.[8] However, the free energy of tautomerization is dependent on the theoretical model adopted for the isolated gas phase calculations. Small variations in $\Delta G_{SH \to NH}$(solv) may lead to large changes in the equilibrium constant, as discussed later.

Once the variation of the enthalpy and the Gibbs free energy were computed for the tautomerization process, $\Delta H_{SH \to NH}$-(solv)= −1.71 kcal/mol and $\Delta G_{SH \to NH}$(solv) = −1.86 kcal/mol, respectively, the entropy contribution can be computed easily using the well-known thermodynamic relation

$$\Delta G_{SH \to NH}(\text{solv}) = \Delta H_{SH \to NH}(\text{solv}) - T\Delta S_{SH \to NH}(\text{solv}) \quad (6)$$

Therefore, the entropy contribution to the tautomerization process of thiol → thione in aqueous solution is $T\Delta S_{SH \to NH}$-(solv) = 0.15 kcal/mol. Equivalent to the gas phase process, this contribution is seen to be very small and does not play a major role in the tautomerization.

The detailed calculations of the relative Gibbs free energy of hydration indicates that the thione Pym-NH form is preferable over the thiol Pym-SH**.** Using the MP4 results for the gas phase process, we suggest a value of ca. 1.9 ± 1.0 kcal/mol. This is not very different from the calculated difference in the enthalpy of hydration, i.e., 1.7± 0.5 kcal/mol.

C. Tautomeric Interconversion Mechanism. In the previous sections we have considered the differential stabilization of the thione Pym-NH and thiol Pym-SH forms both in gas and in aqueous environments without any consideration of the possible mechanism for the tautomeric interconversion. This interconversion is considered now and particular attention is given to the energy barrier between the two tautomeric forms. Two distinct mechanisms for the tautomeric interconversion reaction were investigated: a direct *intramolecular* proton transfer mechanism and a *solvent-assisted* mechanism.

1. Interconversion in the Gas Phase. We first consider the tautomeric interconversion in the gas phase. Figures 2 and 3 show the optimized structures obtained for each mechanism in the gas phase, employing the combined relaxed path method.[23] A summary of the results obtained for the intramolecular and solvent-assisted mechanisms is shown in Table 6 and Figure 4. The intramolecular mechanism (Figure 2) proceeds through a three center transition state, **2b**, with an imaginary frequency of 1465i cm^{-1}, computed at the MP2/6-31++G(d,p). The nuclear displacement associated with this normal mode displays a concerted mechanism in which the S−H bond is breaking and the N−H bond is forming. This mechanism leads to a high energy barrier of 34.4 kcal/mol, relative to the Pym-SH form. In the water-assisted mechanism, the incoming water molecule initially forms a hydrogen-bonded complex with the thiol form **3a**, shown in Figure 3, with the water molecule acting as a hydrogen bond acceptor, relative to the SH group and a hydrogen bond donor, relative to the nitrogen atom. Further interaction leads to the transition state **3b**, with an imaginary

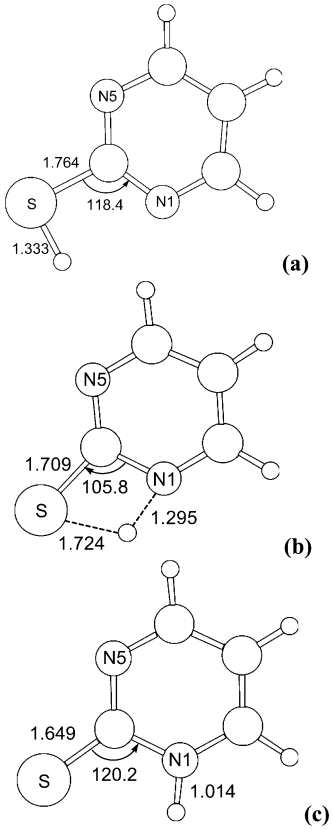

Figure 2. Selected structures obtained along the reaction coordinate for the intramolecular mechanism: (a) thiol form (Pym-SH); (b) transition state (TS); (c) thione form (Pym-NH). Distances are in angstroms and angles in degrees.

frequency of 1443i cm^{-1}, in which a concerted motion of the hydrogen of the SH group and the hydrogen of water takes place. The thione form, **3c**, is then generated as a hydrogen-bonded complex, in which the water molecule now behaves as a hydrogen bond donor, relative to the sulfur atom, and a hydrogen bond acceptor, relative to the NH group. Clearly, the water-assisted mechanism has a smaller potential barrier than the intramolecular mechanism. This water-assisted mechanism has an activation energy of 17.2 kcal/mol, computed at the MP2/6-31++G(d,p), which is half of the value obtained in the intramolecular mechanism. As shown in Figure 4, the relative energy of the tautomers, $\Delta E_{SH\rightarrow NH}$, in the absence of the water molecule, is computed as 7.5 kcal/mol (intramolecular mechanism). In the presence of one water molecule, this relative energy reduces to 2.95 kcal/mol (solvent-assisted mechanism), which represents a considerable reduction of 60% of the $\Delta E_{SH\rightarrow NH}$ in the gas phase.

2. Interconversion in Solution. We now consider the tautomeric interconversion in water. The solvent effects along the reaction pathway for the intramolecular and solvent-assisted mechanisms were analyzed in aqueous solution using the thermodynamic perturbation theory.[15] Each structure obtained in the reaction path of Table 6 and Figure 5 for each mechanism, is perturbed in the subsequent structure along the reaction path, according to eq 1. The LJ parameters of the species are not changed during the perturbation, but the atomic charges of each structure along the reaction path are recomputed using the ChelpG fitting procedure.[22] This allows for the update of the electrostatic interaction between the solute and the water molecules in the reaction path, but it does not update the polarization effect of the solvent in this process. To obtain the

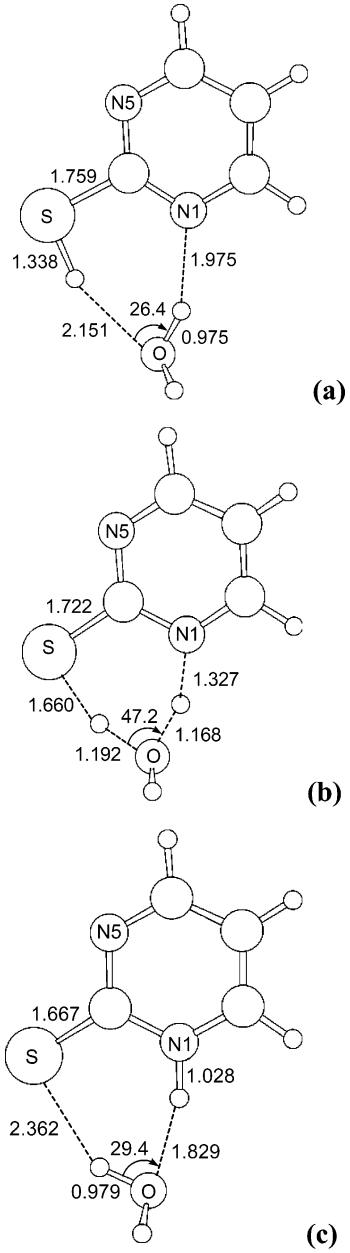

Figure 3. Selected hydrogen-bonded structures obtained along the reaction coordinate for the solvent-assisted mechanism: (a) thiol form (Pym-SH); (b) transition state (TS); (c) thione form (Pym-NH). Distances are in angstroms and angles in degrees.

total free energy difference in solution for the process $i \rightarrow j$, $\Delta G_{SH\rightarrow NH}(solv)$ is written as

$$\Delta G_{i\rightarrow j}(solv) = \Delta G^{XS}_{i\rightarrow j}(solv) + \Delta E_{i\rightarrow j}(gas) \qquad (7)$$

where $\Delta G^{XS}_{i\rightarrow j}(solv)$ is the difference between the species i and j of the solute−solvent term of the free energy in solution obtained with eq 1 and $\Delta E_{i\rightarrow j}(gas)$ is the difference in the intramolecular energies from the ab initio calculations in the gas phase.

For each reaction mechanism, eight simulations using the double-wide sampling were necessary,[15c] to perturb the seventeen points considered in the reaction coordinate. Each simulation consists of a reequilibration phase of 1.8×10^7 MC steps, followed by an average stage of 3.4×10^7 MC steps at the *NpT* ensemble. The results of the solute−solvent term of the free energy in solution are summarized in Table 7, and Figure

TABLE 6: Relative Energy, $\Delta E_{i\rightarrow j}$(gas), Obtained with MP2/6-31++G(d,p) for the Pym-SH → Pym-NH Process Following the Reaction Coordinate in the Gas Phase with the Relaxed Path Algorithm, for the Intramolecular (Figure 2) and the Solvent-Assisted (Figure 3) Mechanisms

	solvent-assisted mechanism		intramolecular mechanism	
P_i	S^a	$\Delta E_{i\rightarrow j}$(gas)	S^a	$\Delta E_{i\rightarrow j}$(gas)
1 (Pym-SH)	−2.33438	0.00	−2.35982	0.00
2	−2.00019	0.49	−2.06563	1.47
3	−1.66700	1.78	−1.77073	4.09
4	−1.33380	4.15	−1.14757	8.01
5	−1.00027	7.71	−1.18042	13.35
6	−0.66681	12.00	−0.88499	20.02
7	−0.33341	15.71	−0.58990	26.99
8	0.00000 (TS)	17.21	−0.29496	32.35
9	0.21560	16.55	0.00000 (TS)	34.40
10	0.43138	14.72	0.24881	32.90
11	0.64710	12.14	0.49499	28.95
12	0.86290	9.44	0.74327	23.92
13	1.07866	7.09	0.99091	19.04
14	1.29441	5.29	1.23858	14.81
15	1.51005	4.05	1.48617	11.43
16	1.72579	3.30	1.73367	8.99
17 (Pym-NH)	1.94182	2.95	1.97978	7.51

[a] The reaction coordinate, S, is presented in (amu)$^{1/2}$ bohr.

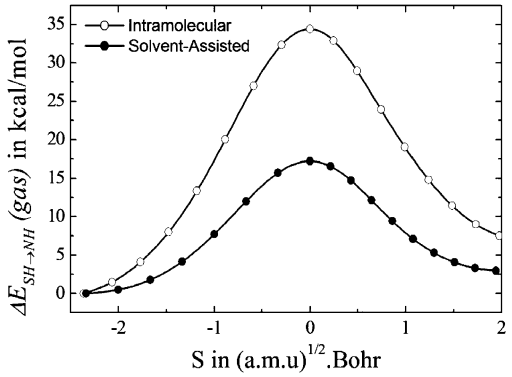

Figure 4. Relative energy in the gas phase obtained with MP2/6-31++G(d,p) for the Pym-SH → Pym-NH process following the reaction coordinate with the relaxed path algorithm, for the intramolecular and the solvent-assisted mechanisms (see Table 6).

5 shows the profile along the reaction coordinate. As can be seen in Figure 5 (top), the intramolecular and solvent-assisted mechanism exhibit similar profiles. In both mechanisms, the transition state ($S = 0$) and the thione-like structures ($S > 0$) are more solvated than the thiol-like structures ($S < 0$). The solvation effects in the transition state are equivalent in both mechanisms, which reduce the transition barrier in approximately 2.4 kcal/mol. At this point the solvent stabilizes more the thione form in the intramolecular mechanism (-6.49 ± 0.58 kcal/mol) than in the solvent-assisted mechanism (-3.27 ± 0.85 kcal/mol). The profile of the total free energy difference in solution for the tautomerization process is obtained using eq 7 and is presented in Figure 5 (bottom). As can be seen, the results clearly indicate that the activation barrier for the water-assisted mechanism is considerably smaller than for the intramolecular process. Although the solvent-assisted mechanism involves a considerably smaller barrier for interconversion, compared to the direct intramolecular mechanism, it should be noted that the barrier is still a pronounced value of 14.8 kcal/mol. This situation differs from early semiempirical studies[12a] on hydroxypyridine that found no barrier. Overall, for each mechanism adopted, the influence of the solvent field is relatively small with increased values close to the final thione product.

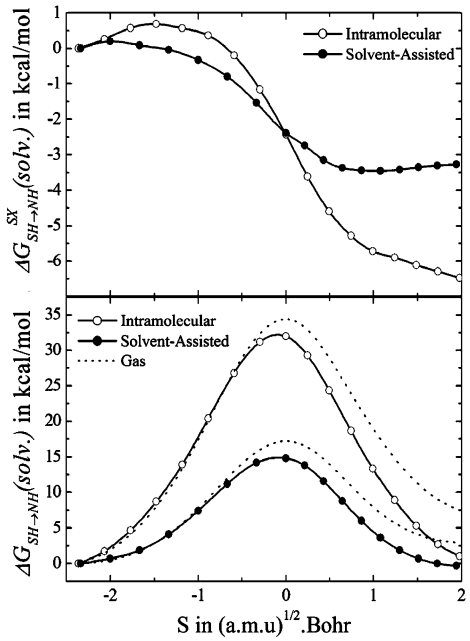

Figure 5. (Top) solute−solvent relative free energy profile and (bottom) total relative free energy profile for the Pym-SH → Pym-NH process following the reaction coordinate with the relaxed path algorithm, for the intramolecular and the solvent-assisted mechanisms.

TABLE 7: Solute−Solvent Gibbs Free Energy Difference (kcal/mol) for the Tautomeric Interconversion (Thiol → Thione) in Water a 25 °C and 1 atm

		solvent-assisted mechanism	intramolecular mechanism
P_i	P_j	$\Delta G^{XS}_{P_i\rightarrow P_j}$(solv)	$\Delta G^{XS}_{P_i\rightarrow P_j}$(solv)
1 (Pym-SH)	2	0.197	0.263
2	3	−0.107	0.314
3	4	−0.129	0.110
4	5	−0.290	−0.116
5	6	−0.470	−0.204
6	7	−0.736	−0.564
7	8	−0.854	−0.962
8	9	−0.355	−1.269
9	10	−0.406	−1.182
10	11	−0.214	−0.983
11	12	−0.074	−0.686
12	13	−0.014	−0.441
13	14	0.034	−0.176
14	15	0.070	−0.213
15	16	0.049	−0.180
16	17 (Pym-NH)	0.032	−0.190
$\Delta G_{SH\rightarrow TS}$(solv)		-2.39 ± 0.43	-2.43 ± 0.29
$\Delta G_{SH\rightarrow NH}$(solv)		-3.27 ± 0.85	-6.49 ± 0.58

P_i's represent each point present on the gas phase reaction path (see Figure 5) starting from the thiol form and ending at the thione form.

But the solvent effect is very important as a participant in the water-assisted mechanism, considerably decreasing the activation barrier. Table 8 summarizes the results for the energetics involved in the thiol → thione conversion, considered here.

D. Analysis of the Tautomerization Constant. The equilibrium constant (in our case, tautomerization constant, K_T) in solution can be evaluated using the expression

$$\Delta G(\text{solv}) = -RT \ln(K_T) \tag{8}$$

As discussed before, there are uncertainties associated with the ΔG(solv) value arising not only from the statistical uncertainties involved in the MC simulations but also mostly in the reference energy used for the gas phase results. Applying the expression

TABLE 8: Summary of the Calculated Relative Gibbs Free Energies and Activation Barriers (kcal/mol) As Obtained from the ab Initio MP4//MP2/6-31++G(d,p) and Monte Carlo Simulations

	gas	solution
$\Delta H_{SH\rightarrow NH}$	8.6	-1.71 ± 0.52
$\Delta G_{SH\rightarrow NH}$	8.3	-1.86 ± 1.03

	Transition State (Activation Barrier)[a]			
	gas		solution	
	IM	WA	IM	WA
$\Delta G_{SH\rightarrow TS}$	34.4	17.2	32.0	14.8

[a] IM stands for intramolecular and WA for the water-assisted mechanisms.

(8) to our calculated values using the gas phase MP4 and MP2 reference results, we obtain $\Delta G_{SH\rightarrow NH}(solv) = -1.86$ and -1.26 kcal/mol, respectively, in aqueous solution, without assuming any mechanism for the tautomerization process. Using these values, we obtain the equilibrium constant as 23 and 8, respectively. This yields an interval of 4−10% of the thiol form present in the aqueous solution. The equilibrium constant for the process Pym-SH → Pym-NH in aqueous solution, is apparently not available experimentally. But for the analogous compound 2-oxopyridine, the tautomerization constant in ethanol is predicted to be larger than 15.[12c] Our results for the tautomerization constant in aqueous solution for the 2-mercaptopyrimidine suggest a value between 8 and 23. However, as can be seen, the equilibrium constant is very sensitive to the value of $\Delta G_{SH\rightarrow NH}(solv)$, which, in turn, depends on the theoretical model employed for the gas phase result.

IV. Summary and Conclusions

Modeling chemical reactions in solution with complete characterization of the free energy surface and mechanistic details is a great challenge. In the present work a combined quantum mechanical and Monte Carlo simulation study was carried out to study the tautomeric equilibrium of 2-mercaptopyrimidine in the gas phase and in aqueous solution. Two tautomers are considered, the thiol and thione forms. The stability of these isolated species, the factors governing the preferential solvation of the species, and hydrogen bond analysis of the solvated tautomers were analyzed.

The studies of the isolated tautomers in the gas phase made at the second- and fourth-order Møller−Plesset theories indicate that the thiol is more stable than the thione by ca. 8 kcal/mol. In aqueous solution, thermodynamic perturbation theory implemented on a Monte Carlo *NpT* simulation indicates that both the differential enthalpy and Gibbs free energy favor the thione form. The calculated differential enthalpy is $\Delta H_{SH\rightarrow NH}(solv) = -1.7$ kcal/mol and the differential Gibbs free energy is $\Delta G_{SH\rightarrow NH}(solv) = -1.9$ kcal/mol.

Analysis of the hydrogen bonds formed between the solutes, thiol and thione, with water indicate that the strength of hydrogen bonds formed are stronger in the case of thione, in line with the stability in aqueous solution.

The tautomeric interconversion along the reaction coordinate was also studied. Two distinct mechanisms were considered: a direct intramolecular proton transfer and a solvent-assisted mechanism. In the gas phase, the intramolecular mechanism leads to an energy barrier of 34.4 kcal/mol, passing through a three-center transition state.The proton transfer with the assistance of one water molecule gives rise to a decreased energy barrier of 17.2 kcal/mol, a reduction of 50% compared with the intramolecular mechanism. The solvation effect decreases the energy barrier on the transition state by 2.4 kcal/mol, both the direct and solvent-assisted paths. The effect of the solvent field along the reaction coordinate is relatively small but the activation barrier in the water-assisted mechanism is considerably smaller compared to the intramolecular mechanism. All theoretical results analyzed here suggest the thione as more stable in water, as indeed inferred experimentally. Finally, the calculated total Gibbs free energy is used to estimate the equilibrium constant.

Summarizing, this work presents the first systematic investigation of the tautomeric equilibrium of 2-mercaptopyridine that includes the statistical and quantum mechanical aspects. We find that thiol is more stable in the gas phase but the thione form is more stable in aqueous solution. Large activation barriers are obtained for the interconversion of one form to the other, and the solvent effect is considerably more important as a participant in the water-assisted mechanism than the solvent field of the solute−solvent interaction. For the interconversion, we find that the solvent-assisted mechanism has an energy barrier that is essentially half of that calculated for the direct intramolecular proton transfer.

Acknowledgment. This work has been partially supported by the Brazilian agencies CNPq and FAPESP. M.C.P.L. also thanks MEC/SESu for an undergraduate scholarship within the PET program.

References and Notes

(1) (a) Robins, P. K. *J. Med. Chem*. **1964**, *7*, 186. (b) Carbon, J. A.; Hung, L.; Jones, D. S. *Proc. Natl Acad. Sci*. **1965**, *53*, 979. (c) Carbon, J. A.; David, H.; Studier, M. H. *Science* **1968**, *161*, 1146. (d) Yu, M. Y. W.; Sedlak, J.; Lindsay, R. H. *Arch. Biochem. Biophys*. **1973**, *155*, 111. (e) Abbot, J.; Goodgame, B. M. L. Jeeves, I. *J. Chem. Soc., Dalton Trans*. **1978**, 880.

(2) (a) Pullman, B.; Pullman, A. *Adv. Heterocycl. Chem*. **1971**, *13*, 77. (b) Kwiatkowski, J. S.; Pullman, B. *Adv. Heterocycl. Chem*. **1975**, *18*, 199. (c) Topal, M. D.; Fresco, J. R. *Nature*, **1976**, *263*, 285. (d) Topal, M. D.; Fresco, J. R. *Nature* **1976**, *263*, 289.

(3) Raper, E. S. *Coord. Chem. Rev*. **1996**, *153*, 199.

(4) (a) Bayon, J. C.; Claver, C.; Masdeu-Bulto, A. M. *Coord. Chem. Rev*. **1999**, *193*, 73. (b) Akrivos, P. D. *Coord. Chem. Rev*. **2001**, 21z3, 181.

(5) (a) Beak, P. *Acc. Chem. Res*. **1977**, *10* 186. (b) Beak, P.; Covington, J. B., White, J. W. *J. Org. Chem*. **1980**, *45*, 1347.

(6) (a) Penfold, B. R. *Acta Crystallogr*. **1953**, *6*, 707. (b) Ohms, U.; Guth, H.; Kutoglu, A.; Scheringer, C. *Acta Crystallogr*. **1982**, *B38*, 831.

(7) Stoyanov, S.; Petkov, I.; Antonov, L.; Stoyanova, T.; Karagiannidis, P.; Aslanidis, P. *Can. J. Chem*. **1990**, *68*, 1482.

(8) Aksnes, D. W.; Kryvi, H. *Acta Chem. Scand*. **1972**, *26*, 2255.

(9) Nowak, M. J.; Rotkowska, H.; Lapinski, L.; Leszczynski, J.; Kwiatkowski, J. S. *Spectrochim. Acta* **1991**, *47A*, 339.

(10) (a) Gronneberg, T.; Undheim, K. *Org. Mass Spectrom*. **1972**, *6*, 823. (b) Maquestiau, A. van Haverbeke, Y.; De Meyer, A.; Katritzky, A. R.; Cook, M. J.; Page, A. D. *Can. J. Chem*. **1975**, *53*, 490.

(11) Cook, M. J.; El-Abbady, S.; Katritzky, A. R, Guimon, C.; Pfister-Guillouzo, G. *J. Chem. Soc., Perkin Trans*. **1977**, *2*, 1652.

(12) (a) Lledós, A.; Bertrán, J. *Tetrahedron Lett*. **1981**, *22*, 775. (b) Scanlan, M. J.; Hillier, I. *Chem. Phys. Lett*. **1984**, *107*, 330. (c) Cieplak, P.; Bash, P.; Singh, U. C.; Kollman, P. A. *J. Am. Chem. Soc*. **1987**, *109*, 6283. (d) Karelson, M. M.; Katrizky, A. R.; Szafran, M.; Zerner, M. C. *J. Org. Chem*. **1989**, *54*, 6030. (e) Katrizky, A. R.; Szafran, M.; Stevens, J. *J. Mol. Struct.* (*THEOCHEM*) **1989**, *184*, 179. (f) Contreras, J. G.; Alderete, J. B. *Chem. Phys. Lett*. **1995**, *232*, 61. (g) Martinez-Merino, V.; Gil, M. J. *J. Chem. Soc., Perkin Trans*. **1999**, *2*, 801. (h) Martos-Calvente, R.; O'shea, V. A. P.; Campos-Martin, J. M.; Fierro, J. L. G. *J. Phys. Chem. A* **2003**, *107*, 7490.

(13) (a) Nesmeyanov, A. N.; Zavelovich, E. B.; Babin, V. N.; Kochetkova, N. S.; Fedin, E. I. *Tetrahedron* **1975**, *31*, 1461. (b) Bensaude, O.; Chevrier, M.; Dubois, J. E. *J. Am. Chem. Soc*. **1978**, *100*, 7055.

(14) Bensaude, O.; Chevrier, M.; Dupois, J. E. *J. Am. Chem. Soc*. **1979**, *101*, 2423.

(15) (a) Zwanzig, R. *J. Chem. Phys*. **1954**, *22*, 1420. (b) Jorgensen, W. L.; Buckner, J. K.; Boudon, S.; Tirado-Rives, J. *J. Chem. Phys*. **1988**, *89*,

3742. (c) Jorgensen, W. L.; Briggs, J. M.; Contreras, M. L. *J. Phys. Chem.* **1990**, *94*, 1683. (d) Straatsma, T. P.; McCammon, J. A. *J. Chem. Phys*. **1989**, *90*, 3300.

(16) (a) Ditchfield, R.; Hehre, W. J.; Pople, J. A. *J. Chem. Phys*. **1971**, *54*, 724. (b) Hehre, W. J.; Ditchfield, R.; Pople, J. A. *J. Chem. Phys*. **1972**, *56*, 2257.

(17) (a) Clark, T.; Chandrasekhar, J.; Spitznagel, G. W.; Schleyer, P. v. R. *J. Comput. Chem*. **1983**, *4*, 294. (b) Frisch, M. J.; Pople, J. A.; Binkley, J. S. *J. Chem. Phys*. **1984**, *80*, 3265.

(18) Allen, M. P.; Tildesley, D. J. *Computer Simulation of Liquids*; Clarendon: New York, 1987.

(19) Metropolis, N.; Rosenbluth, A. W.; Rosenbluth, M. N.; Teller, A. H.; Teller, E. *J. Chem. Phys*. **1953**, *21*, 1087.

(20) Jorgensen, W. L.; Chandrasekhar, J.; Madura, J. D.; Impey, R. W.; Klein, M. *J. Chem. Phys*. **1983**, *79*, 926.

(21) Jorgensen, W. L.; Madura, J. D.; Swenson, C. J. *J. Am. Chem. Soc*. **1984**, *106*, 6638.

(22) Breneman, C. M.; Wiberg, K. B. J. *Comput. Chem*. **1990**, *11*, 361.

(23) Ayala, P. Y.; Schlegel, H. B. *J. Chem. Phys*. **1997**, *107*, 375.

(24) Peng, C.; Schlegel, H. B. *Isr. J. Chem*. **1993**, *33*, 449.

(25) (a) Gonzalez, C.; Schlegel, H. B. *J. Chem. Phys*. **1989**, *90*, 2154. (b) Gonzalez, C.; Schlegel, H. B. *J. Phys. Chem*. **1990**, *94*, 5523.

(26) Frisch, M. J.; Trucks, G. W.; Schlegel, H. B.; Scuseria, G. E.; Robb, M. A.; Cheeseman, J. R.; Zakrzewski, V. G.; Montgomery, J. A., Jr.; Stratmann, R. E.; Burant, J. C.; Dapprich, S.; Millam, J. M.; Daniels, A. D.; Kudin, K. N.; Strain, M. C.; Farkas, O.; Tomasi, J.; Barone, V.; Cossi, M.; Cammi, R.; Mennucci, B.; Pomelli, C.; Adamo, C.; Clifford, S.; Ochterski, J.; Petersson, G. A.; Ayala, P. Y.; Cui, Q.; Morokuma, K.; Malick, D. K.; Rabuck, A. D.; Raghavachari, K.; Foresman, J. B.; Cioslowski, J.; Ortiz, J. V.; Stefanov, B. B.; Liu, G.; Liashenko, A.; Piskorz, P.; Komaromi, I.; Gomperts, R.; Martin, R. L.; Fox, D. J.; Keith, T.; Al-Laham, M. A.; Peng, C. Y.; Nanayakkara, A.; Gonzalez, C.; Challacombe, M.; Gill, P. M. W.; Johnson, B.; Chen, W.; Wong, M. W.; Andres, J. L.; Head-Gordon, M.; Replogle, E. S.; Pople, J. A. *Gaussian 98*, revision A.6; Gaussian, Inc.: Pittsburgh, PA, 1998.

(27) Coutinho, K.; Canuto, S. *DICE: A general Monte Carlo program for liquid simulation*, University of São Paulo, São Paulo, Brazil, 2000.

(28) Kwiatkowski, J. S.; Pullman, B. *Adv. Heterocycl. Chem.* **1975**, *18*, 199.

(29) (a) Guedes, R. C.; Coutinho, K.; Cabral, B. J. C.; Canuto, S. *J. Phys. Chem. B* **2003**, *107*, 4304. (b) Guedes, R. C.; Coutinho, K.; Cabral, B. J. C.; Canuto, S.; Correia, C. F.; Santos, R. M. B.; Martinho Simões, J. A. *J. Phys. Chem. A* **2003**, *107*, 9197.

(30) (a) Stilinger, F. H.; Rahman, A. *J. Chem. Phys*. **1974**, *60*, 3336. (b) Mezei, M.; Beveridge, D. L. *J. Chem. Phys.* **1981**, *74*, 622. (c) Canuto, S.; Coutinho, K. *Int. J. Quantum Chem*. **2000**, *77*, 192. (d) Coutinho, K.; Canuto, S. *J. Chem. Phys*. **2000**, *113*, 9132. (e) Rocha, W. R.; de Almeida, K. J.; Coutinho, K.; Canuto, S. *Chem. Phys. Lett*. **2001**, *345*, 171. (f) Malaspina, T.; Coutinho, K., Canuto, S. *J. Chem. Phys.* **2002**, *117*, 1692. (g) Rocha, W. R.; Martins, V. M.; Coutinho, K.; Canuto, S. *Theor. Chem. Acc*. **2002**, 108, 31 (h) Coutinho, K.; Canuto, S. *J. Mol. Struct. (THEOCHEM)* **2003**, *632*, 235.

(31) Georg, H. C.; Coutinho, K.; Canuto, S. *Chem. Phys. Lett*. **2005**, *413*, 16.